Optimization of stellarator access ports for maintenance

A. Baillod[1] and E. J. Paul[1]

[1]*Department of Applied Physics and Applied Mathematics, Columbia University, New York, New York 10027, USA*

December 22, 2023

Abstract

- MAIS SALUT DIT VOIR

- Future magnetic confinement fusion power plant will require remote maintenance to replace the breeding blanket
- Stellarators have a complex geometry that can be optimized for better accessibility
- In this paper, we describe how the maximum port size can be evaluated given a vessel and the coils geometry
- We show that the port size can be optimized to allow better access to the in-vessel components while keeping the same magnetic field quality
- Three standard stellarators are considered, namely a quasi-axisymmetric, a quasi-helically symmetric and a quasi-isodynamic configuration
- ...

1 Introduction

Core motivation papers are:

- Paper by Bachmann *et.al.* [**bachmann˙2022**] on DEMO remote maintenance system design

- ARIES-CS design paper [**raffray˙2008**] by A. R. Raffray *et.al.*
- Private communication with L. Jorrit

Main points are

- During the lifetime of a reactor, the breeding blanket (BB) will need to be replaced source?
- This maintenance process will have to be done remotely using remote handling (RH) tools
- The complexity of the operation and reactor down-time increases with the number of elements to be replaced
- The number of elements is set by their size, which in turn is set by the size of the port used to access the in-vessel components
- Overall, large ports are desirable

Paper contribution

- Development of a new method to measure the maximum port size
- Application to three different configuration
- Optimization to show that the port size can be increased
- Comparison between QA, QI and QH access?

Paper is organized as follows

- In section 2 we describe how the port size is evaluated given a vessel boundary and the geometry of the coils

2 Port size evaluation

We describe in this section how the port size is evaluated for any given point $\tilde{\mathbf{x}}$ on the vessel boundary δV — here we assume that the surface δV encloses a toroidal volume $\mathcal{V}$, which contains the plasma and blanket, and that the coils are outside $\mathcal{V}$. The idea is to project the vessel boundary and the coils on a plane tangent to the vessel boundary at $\tilde{\mathbf{x}}$. The maximum circular port is then the largest circle centered at $\tilde{\mathbf{x}}$ that fits within the vessel projection and does not intersect any of the projected coils. Not all segments of the coils are of interest though; only segment "in front" of the vessel (this concept will be defined in more details below) have to be taken into account. We will use three different coordinate systems; the first one is the cartesian coordinate system $(\hat{\mathbf{i}}, \hat{\mathbf{j}}, \hat{\mathbf{k}})$, in which the coils, represented as filaments, will be expressed. The second coordinate system is the standard cylindrical coordinate system $(\hat{\mathbf{r}}, \hat{\phi}, \hat{\mathbf{k}})$, which defines the toroidal angle ϕ, and will be used to represent the vessel boundary $\delta\mathcal{V}$. Finally, to evaluate which segment of which coil might get in the way of the access path, we will need a third coordinate system, that we denote $(\hat{\mathbf{n}}, \hat{\mathbf{t}}, \hat{\mathbf{b}})$ and is defined below.

We parametrize the vessel boundary $\delta\mathcal{V}$ by a double Fourier series, $\mathbf{x}^v(\theta,\phi) = R(\theta,\phi)\hat{\mathbf{r}} + Z(\theta,\phi)\hat{\mathbf{k}} \in \delta\mathcal{V}$ with

$$R(\theta,\phi) = \sum_{m=0}^{M}\sum_{n=-N}^{N} R_{mn}\cos(m\theta - nN_f\phi) \tag{1}$$

$$Z(\theta,\phi) = \sum_{m=0}^{M}\sum_{n=-N}^{N} Z_{mn}\sin(m\theta - nN_f\phi), \tag{2}$$

where θ is a poloidal angle, (M, N) are the largest poloidal and toroidal Fourier mode number respectively, (R_{mn}, Z_{mn}) are the Fourier coefficients for the coordinate R and Z respectively, N_f is the number of field period (discrete toroidal symmetry) of the boundary, and stellarator symmetry [**dewar˙1998**] is assumed. We discretize the vessel boundary with a uniform grid in the poloidal and toroidal direction, $\mathbf{x}_i^v = \mathbf{x}^v(\theta_i,\phi_i)$, with $i \in \{1,\dots,N_\theta N_\phi\}$.

Given a point $\tilde{\mathbf{x}} = \mathbf{x}^v(\tilde{\theta},\tilde{\phi})$ on $\mathcal{S}$, we construct the coordinate system $(\hat{\mathbf{n}}, \hat{\mathbf{t}}, \hat{\mathbf{b}})$, with $\tilde{\mathbf{x}}$ as origin, and where $\hat{\mathbf{n}}$ is a unitary vector normal to $\mathcal{S}$ at $\tilde{\mathbf{x}}$, pointing outwards from $\mathcal{V}$, $\hat{\mathbf{t}}$ is a unitary vector tangential to the vessel boundary at $\tilde{\mathbf{x}}$ and pointing in the direction of $\partial\tilde{\mathbf{x}}/\partial\phi$, and $\hat{\mathbf{b}} = \hat{\mathbf{n}} \times \hat{\mathbf{t}}$ (see Figure 1). This coordinate system is nothing else than a rotated and translated cartesian coordinate system, and the coordinates of any point $\mathbf{x} = x_n\hat{\mathbf{n}} + x_t\hat{\mathbf{t}} + x_b\hat{\mathbf{b}}$ are easily obtained by solving the linear system

$$\mathbf{M}(\tilde{\mathbf{x}})\begin{pmatrix} x_n \\ x_t \\ x_b \end{pmatrix} = \mathbf{x} - \tilde{\mathbf{x}}, \tag{3}$$

where $\mathbf{M}$ is a 3×3 matrix with columns set by the vectors $(\hat{\mathbf{n}}, \hat{\mathbf{t}}, \hat{\mathbf{b}})$ written in cartesian coordinates. Once projected on the $(\hat{\mathbf{t}}, \hat{\mathbf{b}})$-plane, the vessel

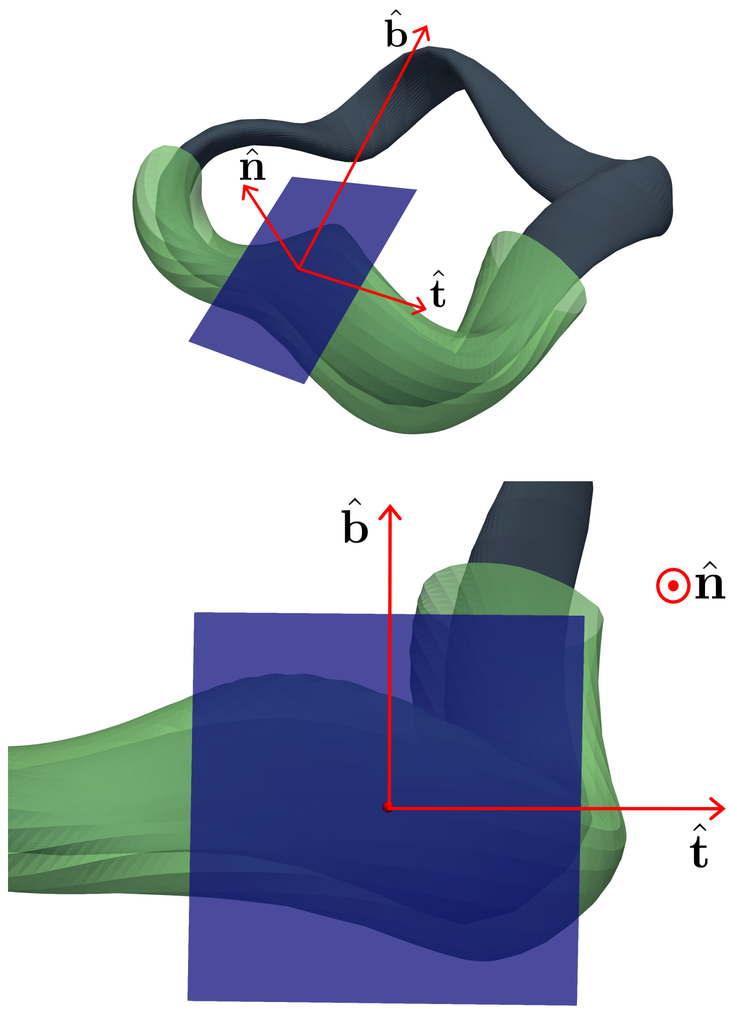

Figure 1: Sketch of the $(\hat{\mathbf{n}}, \hat{\mathbf{t}}, \hat{\mathbf{b}})$ coordinate system. Black toroidal surface: plasma boundary. Green surface: three-halves field period of the vessel boundary $\delta\mathcal{V}$. Blue plane: plane tangent to $\delta\mathcal{V}$ at $\tilde{\mathbf{x}} \in \delta\mathcal{V}$. Top: side view, bottom: front view.

boundary $\delta\mathcal{V}$ is bounded by two curves, that we call the upper envelop $\mathbf{u}(x)$ and lower envelop $\mathbf{l}(x)$. Writing

$$x_b(\theta,\phi) = \left[\mathbf{M}^{-1}(\mathbf{x}^v(\theta,\phi) - \tilde{\mathbf{x}})\right]\cdot\hat{\mathbf{b}} \tag{4}$$

$$x_t(\theta,\phi) = \left[\mathbf{M}^{-1}(\mathbf{x}^v(\theta,\phi) - \tilde{\mathbf{x}})\right]\cdot\hat{\mathbf{t}}, \tag{5}$$

we define

$$\mathbf{u}(x) = u_n(x)\hat{\mathbf{n}} + x\hat{\mathbf{t}} + u_b(x)\hat{\mathbf{b}} \tag{6}$$

$$u_b(x) = \max_{\substack{(\theta,\phi)\in[0,2\pi]\times[0,2\pi/N_f]\\ u_t=\text{const}}} x_b(\theta,\phi), \tag{7}$$

where $u_n(x)$ is chosen such that $\mathbf{u}\in\partial\mathcal{V}$. Similarly,

$$\mathbf{l}(x) = l_n(x)\hat{\mathbf{n}} + x\hat{\mathbf{t}} + l_b(x)\hat{\mathbf{b}} \tag{8}$$

$$l_b(x) = \min_{\substack{(\theta,\phi)\in[0,2\pi]\times[0,2\pi/N_f]\\ u_t=\text{const}}} x_b(\theta,\phi). \tag{9}$$

The curves $u_b(x)$ and $l_b(x)$ form the non-convex hull of the vessel boundary projected on the $(\hat{\mathbf{t}},\hat{\mathbf{b}})$-plane (see Figure 2), and are evaluated using the χ-algorithm proposed by M. Duckham *et.al.* [**duckham˙2008**]. The maximum port size around $\tilde{\mathbf{x}}$ is set by the minimal distance to the upper or lower envelop,

$$r_{port}^{lim} = \min_x[\mathbf{u}(x)\cdot\hat{\mathbf{b}}, \mathbf{l}(x)\cdot\hat{\mathbf{b}}]. \tag{10}$$

Note that the maximum port size defined by Eq.(22) depends on the position of the port $\tilde{\mathbf{x}}$.

We now consider N_{coils} coils, that we represent by filaments Γ_j (curve of zero width) in cartesian coordinates. We express their position as Fourier series as proposed by Zhu *et.al.* [**zhu˙2017**], $\mathbf{x}^c(l) = x^c(l)\hat{\mathbf{i}} + y^c(l)\hat{\mathbf{j}} + z^c(l)\hat{\mathbf{k}}$, where

$$x^c(l) = x^c_{e,0} + \sum_{k=1}^{N_k} x^c_{e,1}\cos(2\pi kl) + \sum_{k=1}^{N_k} x^c_{o,1}\sin(2\pi kl) \tag{11}$$

$$y^c(l) = y^c_{e,0} + \sum_{k=1}^{N_k} y^c_{e,1}\cos(2\pi kl) + \sum_{k=1}^{N_k} y^c_{o,1}\sin(2\pi kl) \tag{12}$$

$$z^c(l) = z^c_{e,0} + \sum_{k=1}^{N_k} z^c_{e,1}\cos(2\pi kl) + \sum_{k=1}^{N_k} z^c_{o,1}\sin(2\pi kl), \tag{13}$$

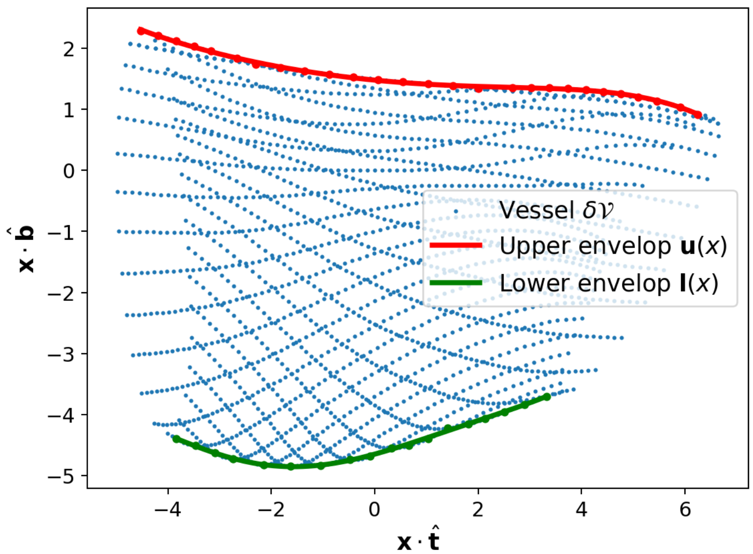

Figure 2: Vizualization of the upper and lower envelop, $\mathbf{u}(x)$ and $\mathbf{l}(x)$, as defined by Eqs.(6)-(9).

with $l \in [0,1]$. Each coil filament is then discretized in N_p quadrature points $(x_p^c, y_p^c, z_p^c) = (x^c(l_p), y^c(l_p), z^c(l_p))$, with $l_p = (p-1)/N_p$, $p \in \{1,\ldots,N_p\}$. We pack all coils quadrature points in a single array of size $N_{coils}N_p$, and denote by $\mathbf{x}_i^c$ their position. Again, solving Eq.(3) provides the coils quadrature points coordinate in the $(\hat{\mathbf{n}}, \hat{\mathbf{t}}, \hat{\mathbf{b}})$ coordinate system (see Figure 3),

$$\mathbf{x}_i^c = x_i^c\hat{\mathbf{i}} + y_i^c\hat{\mathbf{j}} + z_i^i\hat{\mathbf{k}} = n_i^c\hat{\mathbf{n}} + t_i^c\hat{\mathbf{t}} + b_i^c\hat{\mathbf{b}}. \quad (14)$$

Now, we consider only coil elements standing in front of the vessel, *i.e.* points that satisfy the following conditions (see Figure 4):

1. The point is below the upper envelop, $b_i^c \leq b_i^u$
2. The point is above the lower envelop, $b_i^c \geq b_i^l$
3. If $b_i^c > 0$, the point needs to be in front of $\mathbf{u}(t_i^c)$, *i.e.* $n_i^c \geq n_i^u$
4. If $b_i^c < 0$, the point needs to be in front of $\mathbf{l}(t_i^c)$, *i.e.* $n_i^c \geq n_i^l$

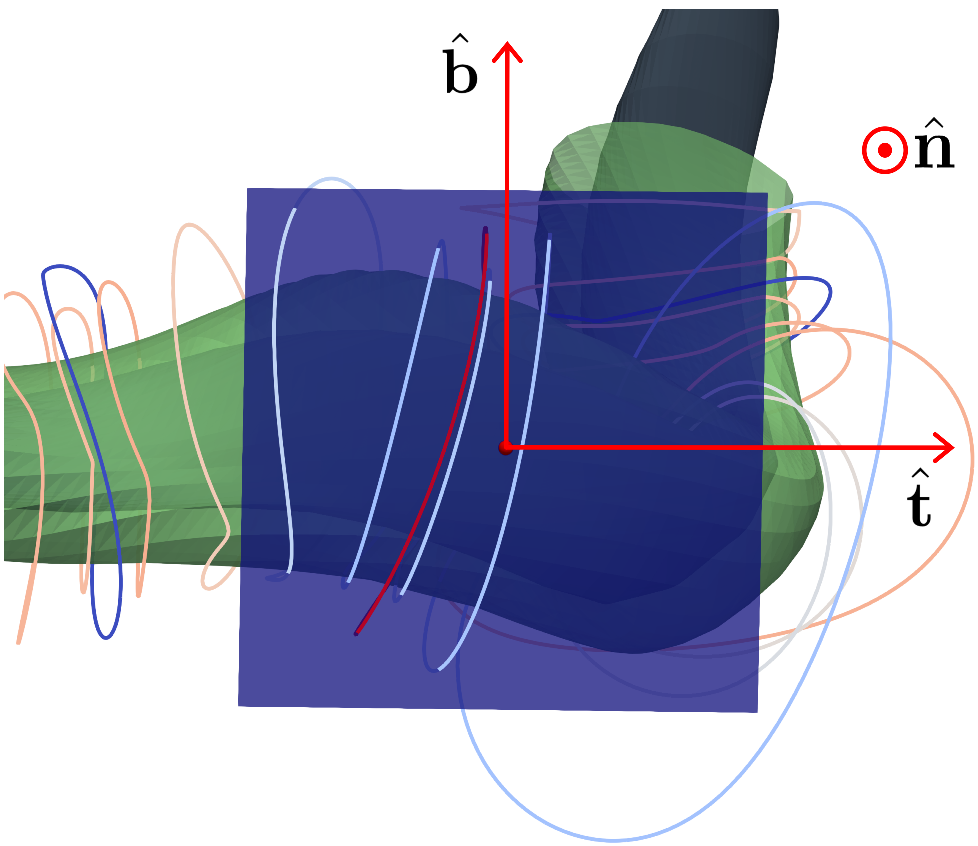

Figure 3: Front view of the plasma surface, vessel and coils.

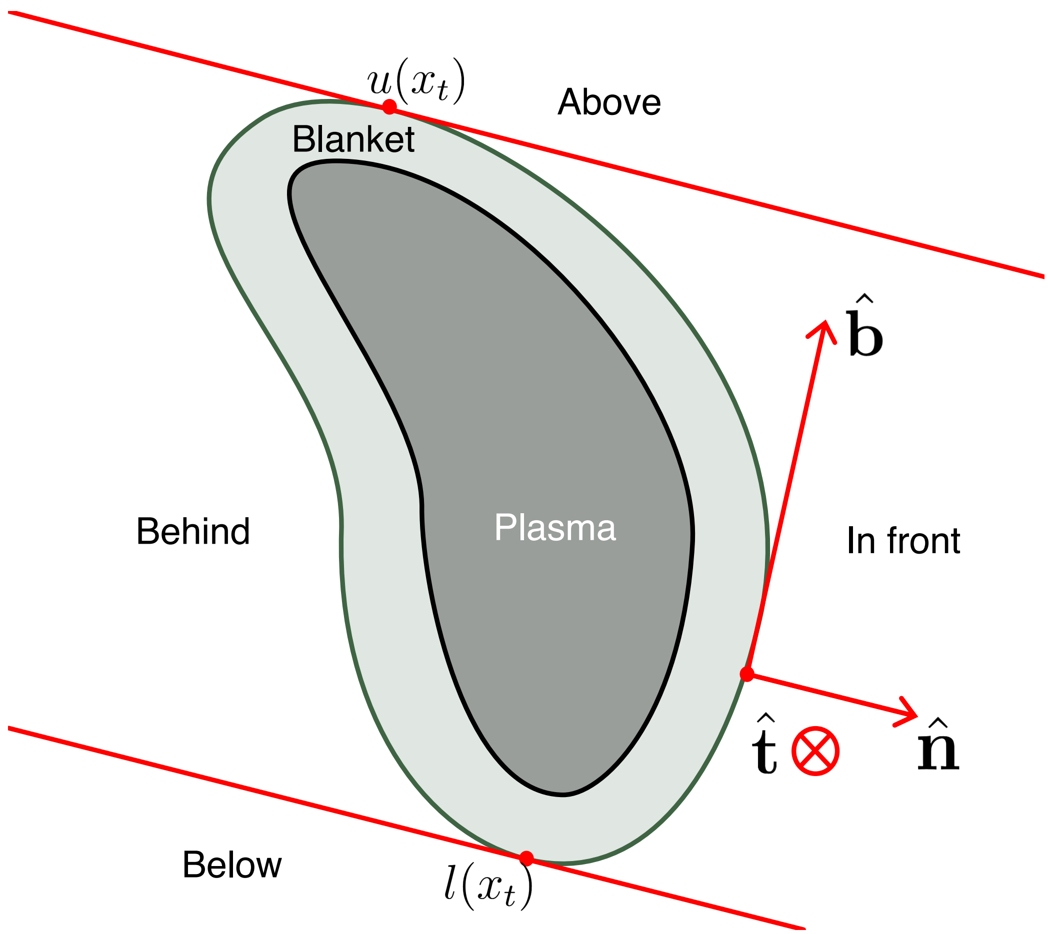

Figure 4: Sketch of coil elements that are in front, above, behind, or below the vessel.

where we used the notation

$$b_i^u = \mathbf{u}(t_i^c) \cdot \hat{\mathbf{b}} \tag{15}$$
$$b_i^l = \mathbf{l}(t_i^c) \cdot \hat{\mathbf{b}} \tag{16}$$
$$n_i^u = \mathbf{u}(t_i^c) \cdot \hat{\mathbf{n}} \tag{17}$$
$$n_i^l = \mathbf{l}(t_i^c) \cdot \hat{\mathbf{n}}. \tag{18}$$

For each point $\mathbf{x}_i^c$, we then evaluate

$$\Lambda(\mathbf{x}_i^c, \tilde{\mathbf{x}}) = \mathcal{H}(b_i^u - b_i^c)\mathcal{H}(b_i^c - b_i^l)) \left\{ \mathcal{H}(-b_i^c)\mathcal{H}(n_i^c - n_i^l) + \mathcal{H}(b_i^c)\mathcal{H}(n_i^c - n_i^u) \right\}, \tag{19}$$

where $\mathcal{H}$ is the Heaviside function, and $\Lambda = 1$ if conditions (1)-(4) are satisfied, and $\Lambda = 0$ otherwise. Then,

$$d_i = k\left[\Lambda(\mathbf{x}_i^c, \tilde{\mathbf{x}}) - 1\right]\sqrt{(b_i^c)^2 + (t_i^c)^2}, \tag{20}$$

where k is a parameter. The metric d_i is then equal to the distance from $\tilde{\mathbf{x}}$ to $\mathbf{x}_p$ in the $(\hat{\mathbf{t}}, \hat{\mathbf{b}})$-plane if conditions (1)-(4) are satisfied, and is equal to a number of the order of k otherwise. The maximum port size is then given by

$$r_{port}(\tilde{\mathbf{x}}) = \min\{r_{port}^{lim}, \min_{i \in \{1,\dots,N_{coils}N_{pts}\}} d_i\}. \tag{21}$$

Finally, the maximum port size on the vessel boundary is obtained by taking the maximum over (θ, ϕ),

$$r_{port}^{max} = \max_{(\theta,\phi)\in[0,2\pi]\times[0,2\pi/N_f]} r_{port}(\tilde{\mathbf{x}}(\theta,\phi)). \tag{22}$$

In practice, we limit the search to regions facing the outboard side of the device, by constraining the poloidal angle to remain within some bounds, $\theta \in [-\pi/2, \pi/2]$.

To allow optimization of the maximum port size, Eq.(22), the metric r_{port}^{max} needs to be differentiable with respect to the coils degrees of freedom, *i.e.* the coils Fourier harmonics. This property is achieved by approximating the maximum and minimum functions in Eq.(21) by the p-norm,

$$||\{f_i\}||_p \approx \left[\sum_i f_i^p\right]^{1/p}, \tag{23}$$

with $\min_i f_i \approx ||\{f_i\}||_p$ for $p \ll -1$ and $\max_i f_i \approx ||\{f_i\}||_p$ for $p \gg 1$, and approximating the Heaviside functions in Eq.(19) by the logistic function,

$$\mathcal{H}(x) \approx \frac{1}{2} + \frac{1}{2}\tanh(kx), \tag{24}$$

with $k \gg 1$.

3 Optimiziting stellarator coils for large port size

3.1 Stage II optimization

To optimize the port size of a given configuration, we first start by a standard stage-II optimization. A coil set is sought that accurately reproduce the plasma boundary, *i.e.* where the magnetic field produced by the coils normal to the target plasma boundary is small. This is obtained by minimizing the quadratic flux

$$\psi_n(\boldsymbol{\chi}, \mathbf{I}) = \frac{1}{2}\int_S (\mathbf{B}\cdot\hat{\mathbf{n}})^2 ds, \tag{25}$$

where S is the plasma boundary, and here $\hat{\mathbf{n}}$ refers to the surface unit normal vector. The array $\boldsymbol{\chi}_i$ is an array containing all the curve Γ_i degrees of freedom, and I_i is the current in the coil described by Γ_i. The vector $\boldsymbol{\chi}$ contains the degrees of freedom of all the coils, and the vector $\mathbf{I}$ contains the current from all the coils. In addition, constraints on the coils length L_j, the toroidal flux ψ_t, the coil-to-coil distance d_{cc} and the coil-to-plasma distance d_{cs} are enforced, with

$$L_i(\boldsymbol{\chi}_i) = \max\left(\int_{\Gamma_i} dl - L_0, 0\right)^2 \tag{26}$$

$$P_{\psi_t}(\boldsymbol{\chi}, \mathbf{I}) = \left(\int_{S_\varphi} \mathbf{B}(\boldsymbol{\chi}, \mathbf{I})\cdot\mathbf{n}\ ds - \psi_{t,0}\right)^2 \tag{27}$$

$$d_{cc}(\boldsymbol{\chi}) = \sum_{i=1}^{N_{coils}}\sum_{j=1}^{i-1}\int_{\Gamma_i}\int_{\Gamma_j} \max(d_{cc,0} - \|\mathbf{r}_i - \mathbf{r}_j\|_2, 0)^2\ dl_j\ dl_i \tag{28}$$

$$d_{cs}(\boldsymbol{\chi}) = \sum_{i=1}^{N_{coils}}\int_{\Gamma_i}\int_S \max(d_{cs,0} - \|\mathbf{r}_i - \mathbf{s}\|_2, 0)^2\ dl_i\ ds \tag{29}$$

where The scalar L_0 is the maximum length for a coil, $\psi_{t,0}$ is the target toroidal magnetic flux, $d_{cc,0}$ is the maximum coil-to-coil distance, and $d_{cs,0}$ is the maximum coil-to-surface distance. The full objective function is then

$$f_1(\boldsymbol{\chi}, \mathbf{I}) = \psi_n + w_l \sum_{i=1}^{N_{coils}} L_i + w_t P_{\psi_t} + w_{cc} d_{cc} + w_{cs} d_{cs}, \tag{30}$$

where $(w_l, w_t, w_{cc}, w_{cs})$ are user-supplied weights, and the dependence on $\boldsymbol{\chi}$ and $\mathbf{I}$ have been dropped on the right-hand-side. There are no ways to know what choice of weights will lead to the best results *a priori* — instead, in all results presented in this paper, we scanned various combination of weights until finding satisfactory results. We use the simsopt python framework for stellarator optimization [**landreman˙2021**] to drive the optimization

3.2 Port size optimization

After completing the stage II optimization, we maximize the port size defined in Eq.(22) while keeping the quadratic flux (25) below a threshold $\psi_{n,0}$. To do so, we define the penalty

$$P_{\psi_n}(\boldsymbol{\chi}, \mathbf{I}) = \max(\psi_n - \psi_{n,0}, 0)^2, \tag{31}$$

and we minimize

$$f_2(\boldsymbol{\chi}, \mathbf{I}) = -r_{port}^{max} + w_n P_{\psi_n} + w_l \sum_{i=1}^{N_{coils}} L_i + w_t P_{\psi_t} + w_{cc} d_{cc} + w_{cs} d_{cs}, \tag{32}$$

where w_n is a user-supplied weight, and the dependence on $\boldsymbol{\chi}$ and $\mathbf{I}$ have been dropped. Again, we scan various value for the weight w_n until satisfactory results are obtained. Finally, the metric (22) is implemented usind the JAX python library for automatic differentiation [**jax2018github**], providing derivatives of r_{port}^{max} with respect to the coils degrees of freedom at a fraction of the computational needed to evaluate the derivatives of r_{port}^{max} using finite differences.

Acknowledgements

- L. Jorrit, M. Zarnstoff, J. Schwartz, M. Churchill useful discussion